Scripta METALLURGICA Vol. 15, pp. 287-292, 1981 Pergamon Press Ltd.
Printed in the U.S.A.

TRANSFORMATION PSEUDOELASTICITY AND DEFORMATION BEHAVIOR IN A Ti-50.6at%Ni ALLOY

S.Miyazaki*, K.Otsuka* and Y.Suzuki**

* Institute of Materials Science, University of Tsukuba, Sakura-mura, Ibaraki-ken 305, Japan
** Central Research Laboratory, Furukawa Electric Company, 2-9-15 Futaba-cho, Shinagawa-ku, Tokyo 141, Japan

(Received November 22, 1980)
(Revised December 22, 1980)

Introduction

The Ti-Ni alloy is so famous with the associated shape memory effect. In fact it is the only alloy which is used for the practical applications of the shape memory effect on a commercial basis at present, such as coupling, connectors and medical applications (1). In order to develop such applications, it is necessary to investigate mechanical behavior associated with the martensitic transformation and/or in the martensitic state. Various investigations have been made along this line so far, but the number and scope of these investigations are not very many nor so deep from a fundamental point of view. Rozner and Wasilewski (2), and Cross et al. (3) made rather systematic works on the stress-strain curves (S-S curves) in wide temperature and strain ranges. They found that the S-S curves in the Ti-Ni alloys consisted of three stages which are apparantly similar to three stages in FCC and HCP single crystals. However, they did not study the unloading process, and did not clarify the nature of these stages. The presence of the transformation pseudoelasticity (4) in Ti-51at%Ni and Ti-52at%Ni alloys has been reported by Wasilewski (5) and Honma (6) respectively, but no detailed data such as the temperature dependence etc. have been reported. The purpose of the present short note is to report the transformation pseudoelasticity in this alloy in some detail, and to clarify the nature of the three stages by carefully observing the stress-strain curves upon loading and unloading and by measuring the strains recovered upon unloading and subsequent heating.

After the pioneering works by Rozner and Wasilewski, and Cross et al., several investigations have been made to clarify the nature of each stage. Although it is not well established as yet, we summarize those in the following. Mohamed and Washburn (7) have provided evidence that the martensite-martensite interface moves in the early stage (stage I) of an initially partially transformed material. Some authors (7,8) have suggested that the deformation in stage II is an elastic deformation of the martensites formed in stage I. But Melton and Mercier (9) reported evidence inconsistent with the above suggestion. They observed microstructure in a specimen deformed into stage II by transmission electron microscopy and found an intersecting array of martensite laths in some part and dislocations in another part. However, their observation is limited to a small region of stage II, and the deformation modes throughout the stage II are not well clarified. On stage III, Mohamed and Washburn (7) made an electron microscopy observation of specimens elongated by 8% and found heavy irregularity of martensite boundaries. Thus they suggested that slip occurred at the stage III. Michael (10) and Tadaki and Wayman (11) also made the electron microscopy observation of heavily cold-rolled (≈30%) specimens, which roughly corresponded to stage III in tensile tests. They both found high density of dislocations and the segmentation of martensites. These results are clear evidence to show that slip occurs in stage III, but are lacking for the qualitative data by tensile tests as to the recovery of strains. Meanwhile, apparently quite similar three stage stress-strain curves are reported in Cu-Al-Ni single crystals in specific orientations; the deformation modes in stages II and III in this case are proved unambiguously to be due to the elastic deformation of a martensite and martensite-to-martensite transformation, respectively, by careful measurement of strains by extensometer and neutron diffraction under stress (4). It is interesting to compare the nature of the three stages in the Ti-Ni alloy with those in the above case.

0036-9748-81/030287-06$02.00/0

Experimental Procedures

The alloy was prepared from 99.7wt% Ti and 99.97wt% electrolytic Ni by melting in a high-frequency vacuum induction furnace, followed by casting into an iron mold. The composition of the alloy was determined by chemical analysis to be Ti-50.6at%Ni (±0.1at%Ni) (nominal composition was Ti-51at%Ni). The ingot of the alloy was swaged at R.T. and then drawn at R.T. to wire specimens with the diameter of 0.4 mm. The specimens were solution treated at 1273 K for 1 hr in a vacuum of 10^{-3} Pa, and then rapidly quenched into ice water. The transformation temperatures after this heat treatment were measured by electrical resistance method, and the M_f, M_s, A_s and A_f temperatures were 126, 190, 188 and 221 K, respectively. After these heat treatments, wire specimens with the diameter of 0.35 mm and with gauge length of 16 mm long were made by electropolishing in a solution of acetic anhydride and 7.5% perchloric acid. Tensile tests were carried out with an Instron type tensile machine Shinko TOM-10000X. For testing at various temperatures, the specimens were kept in a solution of methanol or isopentane which was cooled by pouring liquid nitrogen. The strain rate used was 5.2×10^{-4}/sec.

Results and Discussion

(1) Effect of deformation temperature on stress-strain curves

The deformation modes of materials which exhibit thermoelastic martensitic transformations are affected strongly by deformation temperature (T). Such stress-strain curves as a function of temperature are shown in Fig.1. These curves are divided into four temperature regimes as follows according to the characteristics of the curves. In range (I) ($T<M_s$) the curves (a)~(e) are characterized by smooth and parabolic curves. The flow stress increases with decreasing temperature in this range, because the deformation in this range proceeds with the movement of mobile defects such as boundaries between martensite plates or internal twins which move by a thermal activation process.

In range (II) ($M_s<T<A_f$) the curves are characterized by a sharp bending at the yield point, where the apparent plastic deformation starts by the formation of stress-induced martensite (SIM). The serration of curve (h) corresponds to the formation of SIM. Although curves (f) and (g) also belong to range (II), both curves do not show the serration. This may be due to the easiness of the formation of SIM at low stress. The common feature of the curves in both ranges (I) and (II) are characterized by the presence of residual strain after unloading and perfect recovery of the strain after heating, i.e. the specimen shows the shape memory effect in these temperature ranges.

The curves in the third temperature range ($A_f<T<T_d$) are characterized by the formation of SIM upon loading and by the reversible reverse transformation upon unloading, which leads to the transformation pseudoelasticity. Here T_d represents the critical temperature where the plastic deformation by dislocation motion starts. The stress hysteresis of the curves are almost the same in this range and the stress level increases with increasing temperature, according to the Clausius-Clapeyron relation.

In range (IV) ($T_d<T$) the curves are characterized by plastic deformation preceding the formation of SIM as is evident from the deviation from linearity before serration occurs. As expected from the Clausius-Clapeyron equation, the critical stress required to induce martensitic transformation in this temperature range becomes so large that the plastic deformation by the movement of dislocations occurs prior to the formation of SIM. Curve (n) is a typical example of such a case. The slip deformation induced in this range is the cause of the presence of residual strain after unloading which increases with increasing temperature as shown in Fig. 1(m)~(p). It is noted in the S-S curves (n)~(p) that the serrations are present upon loading but they are difficult to detect upon unloading. The serration in general is caused by the deformation in which the deformation unit is large enough and the deformation process is so rapid (12). Therefore the smoothness of the curve during reverse transformation upon unloading implies that the transformation unit has become small and the transformation process has been decelerated owing to the dislocation obstacles which are formed upon loading. Although the behavior in this range is very interesting, it is difficult to make a quantitative analysis from the present data, which has been taken for a single specimen.

(2) Temperature dependence of critical stresses for stress-induced transformation ($T>M_s$) and for yielding ($T<M_s$).

As mentioned in the previous section, the temperature dependence of the yield stress is very complex because the deformation modes differ with each other in the four temperature regions. The critical stresses are plotted in Fig. 2 as a function of temperature. Open circles indicate the stresses at which martensites are induced when $M_s<T$ or boundaries between martensites or

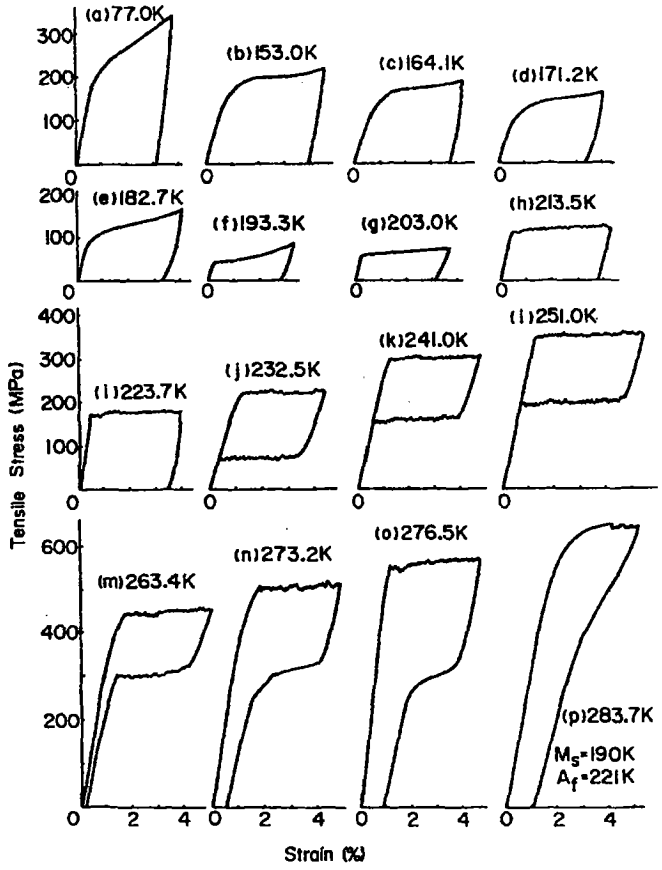

FIG. 1

Stress-strain curves as a function of temperature.

internal twin boundaries begin to move when $T<M_s$. Closed circles show the stresses at which reverse transformation starts. The critical stress takes the minimum value near the M_s point and increases with decreasing temperature in the range below the M_s point. At temperatures above the M_s point, the critical stress increases with increasing temperature, and it satisfies the Clausius-Clapeyron relation between 210 and 260 K. At temperatures above 260 K, where residual strain remains after unloading, both the critical stresses for inducing martensites and reverse transformation deviate from the relation, but the former deviates to the upper side while the latter to the lower side of the relation.

(3) Deformation mode in each stage of the stress-strain curves

The deformation modes are strongly affected not only by the deformation temperature as shown in Fig. 1 but also by the amount of strain. In this section the deformation modes of both specimens which are in a parent phase and in partially martensitic state prior to deformation are examined.

Figure 3 shows the stress-strain curves of a specimen deformed at 243 K ($>A_f$), where the specimen was in parent phase prior to deformation. The specimen was subjected to cyclic stressing as shown by curves 1~9. If there is residual strain after unloading, the specimen was

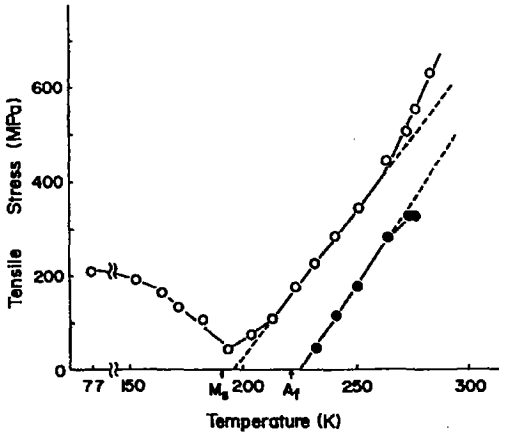

FIG. 2

Critical stresses as a function of temperature for inducing matensites ($T>M_s$) and for yielding ($T<M_s$) (open circles) and for reverse transformation (solid circles).

heated to 373 K in order to recover the residual strain as shown by dotted lines. The stress-strain curve can be divided into three stages conventionally. In stage I, this material shows Lüders like deformation until about 7% strain as shown by curves 1~3. The serrations during the deformation were caused by the formation of SIM. The amount of strain by SIM upon loading is the same as that recovered by reverse transformation upon unloading. This fact shows that all the deformation in this stage is proceeded by the formation of SIM alone.

After the Lüders like deformation the flow stress increases rapidly with increasing strain in the stage II as shown by curves 4~7. When the specimen was deformed to this stage, the strain is not recovered completely upon unloading and even after heating. The existence of residual strain means that plastic deformation by the movement of lattice defects such as dislocations occurs as one of the deformation modes in this stage. By comparing the strain of the serrated region in stage I (ε_s) with the sum of the strain recovered by unloading and that by the subsequent heating (ε_r), it is found that the latter (≈6%) is larger than the former (≈5%) when the specimen is deformed into stage II as shown by curves

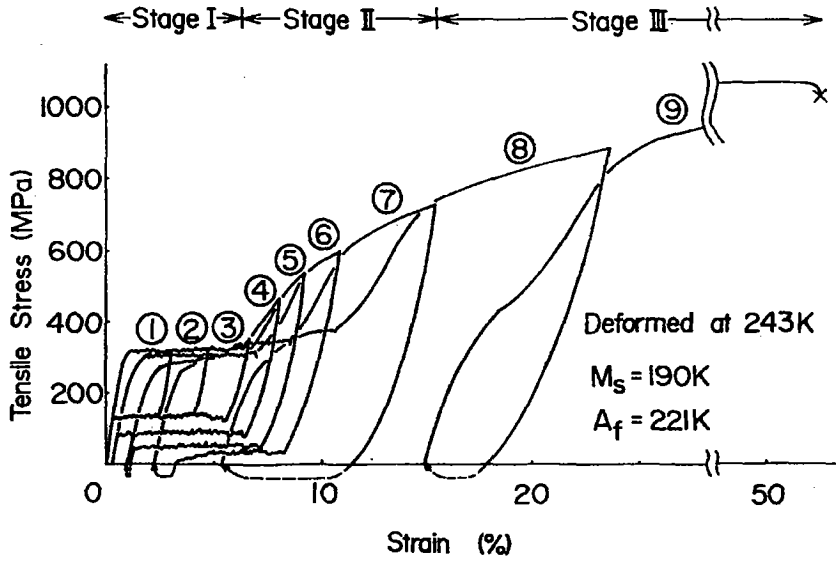

FIG. 3

Stress-strain curves of a specimen deformed at 243 K ($>A_f$). Dotted lines represent the recovered strain upon heating to 373 K. The symbol (×) represents the fracture point.

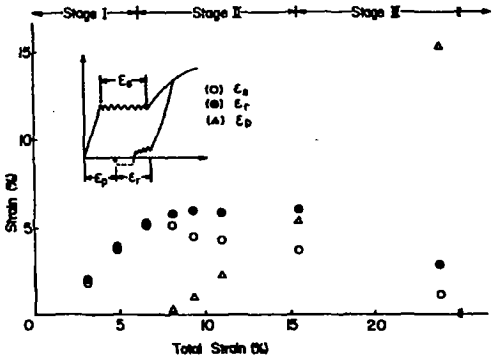

FIG. 4

Plot of various strains as a function of total tensile strain in a specimen deformed at 243 K ($>A_f$).

4-6. These facts mean that there are two deformation modes in the second stage, i.e. the normal plastic deformation by the movement of dislocations and the formation of SIM in the residual parent phase and/or the deformation by the movement of martensite-martensite boundaries and twin boundaries. As these two deformation modes coexist in stage II, the SIM and dislocations relax the strain fields formed by them to each other and the stress field formed by the dislocations makes the martensite stabler. As a consequence, both critical stresses for inducing martensites and for the reverse transformation decrease with increasing strain as shown in Fig. 3.

In stage III the strain ε_r recovered by reverse transformation rapidly decreases and the residual strain (ε_p) after heating to 373 K increases rapidly as shown by curve 8, so that most of the deformation mode in stage III is plastic deformation by the movement of dislocations. Thus it is quite unlikely that the stage III is associated with a martensite-to-martensite transformation, in spite of the great similarity to that of Cu-Al-Ni single crystal in the S-S curves upon loading.

These three kinds of strains ($\varepsilon_s, \varepsilon_r$, and ε_p) in the specimen used in Fig.3 are plotted as a function of total tensile strain in Fig. 4. These strains are defined schematically in Fig. 4. It is found that the residual strain (ε_p) appears at about 8% strain in stage II. This means that the deformation mode up to the initial region of stage II is the formation of SIM or the movement of bounderies of martensites or twin boundaries in martensites and does not contain the movement of dislocations.

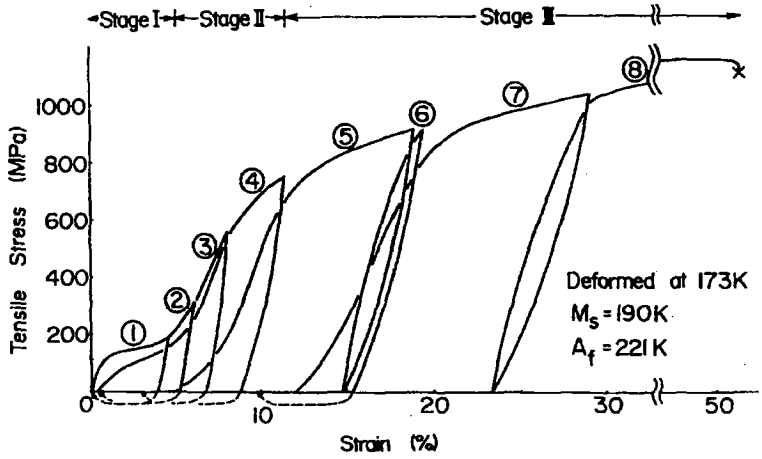

FIG. 5

Stress-strain curves of a specimen deformed at 173 K ($<M_s$). Dotted lines represent the recovered strain upon heating to 373 K. The symbol (×) represents the fracture point.

DOCKET ALARM

Explore Litigation Insights

Docket Alarm provides insights to develop a more informed litigation strategy and the peace of mind of knowing you're on top of things.

Real-Time Litigation Alerts

Keep your litigation team up-to-date with **real-time alerts** and advanced team management tools built for the enterprise, all while greatly reducing PACER spend.

Our comprehensive service means we can handle Federal, State, and Administrative courts across the country.

Advanced Docket Research

With over 230 million records, Docket Alarm's cloud-native docket research platform finds what other services can't. Coverage includes Federal, State, plus PTAB, TTAB, ITC and NLRB decisions, all in one place.

Identify arguments that have been successful in the past with full text, pinpoint searching. Link to case law cited within any court document via Fastcase.

Analytics At Your Fingertips

Learn what happened the last time a particular judge, opposing counsel or company faced cases similar to yours.

Advanced out-of-the-box PTAB and TTAB analytics are always at your fingertips.

API

Docket Alarm offers a powerful API (application programming interface) to developers that want to integrate case filings into their apps.

LAW FIRMS
Build custom dashboards for your attorneys and clients with live data direct from the court.

Automate many repetitive legal tasks like conflict checks, document management, and marketing.

FINANCIAL INSTITUTIONS
Litigation and bankruptcy checks for companies and debtors.

E-DISCOVERY AND LEGAL VENDORS
Sync your system to PACER to automate legal marketing.